Journal of Photochemistry, 11 (1979) 53 - 68

THE ENHANCEMENT EFFECTS OF ATOMIC OXYGEN ON NITRIC OXIDE β BAND CHEMILUMINESCENCE

I. M. CAMPBELL and R. S. MASON*
School of Chemistry, The University, Leeds, LS2 9JT (Gt. Britain)
(Received November 7, 1978)

Summary

In the afterglow associated with combining $N(^4S) + O(^3P)$ atoms, the intensities of β band emissions from $NO(B^2\Pi)v' = 1,2$ show a more than first order dependence on [O]. It is shown that this results from two independent mechanisms populating these levels. One is the accepted general mechanism which also populates $v' = 0, 3$ and involves the intermediate states $NO(a^4\Pi)$ and $NO(b^4\Sigma^-)$. The other, termed the enhancement route, depends strongly upon near-resonant energy transfer processes which are the origin of its specificity. The primary step is a transfer of energy from $NO(a^4\Pi)$ to $N(^4S)$ to produce predominantly $N(^2P)$. $N(^2P)$ combines with $O(^3P)$ and after energy degradation this is postulated to populate a precursor state which, after near-resonant energy transfer to $O(^3P)$ to yield $O(^1D)$, populates NO $(B^2\Pi)v' = 1, 2$.

Identification of the immediate precursor as $NO(B'^2\Delta)$ is shown to explain the specificity of the enhancement route in terms of the resonant nature of the energy transfer processes. It is shown that the intensities of β band emissions require at least 4% of N + O + M combinations to follow the enhancement route.

It is also shown that energy resonance considerations explain the facts that emission from $NO(B^2\Pi)v' = 0$ is predominantly quenched by direct interaction of $O(^3P)$ atoms and by interaction of $N(^4S)$ atoms with the immediate precursor $NO(b^4\Sigma^-)v' = 0$.

1. Introduction

The chemiluminescence associated with the combination of $N(^4S)$ and $O(^3P)$ atoms is evident as a blue colouration due to NO β bands emitted in the transition $B^2\Pi \rightarrow X^2\Pi$. We have recently [1] given an account of the general mechanism by which $NO(B^2\Pi)$ is generated and in particular the immediate precursors to each $NO(B^2\Pi)$ vibrational level were identified as specific vibrational levels of $NO(b^4\Sigma^-)$ with near-resonant energies. In

*Present address: Department of Chemistry and Molecular Sciences, The University of Warwick, Coventry CV4 7AL, Gt. Britain.

order to explain both the kinetic behaviour and the measured intensity distribution of the Ogawa bands ($b^4\Sigma^- \rightarrow a^4\Pi$) also emitted, it was proposed that there were six vibrational levels of $NO(b^4\Sigma^-)$ below the first dissociation limit of NO. Another paper [2] published almost simultaneously and describing electron impact spectroscopic experiments on NO confirmed the proposed vibrational numbering scheme for $NO(b^4\Sigma^-)$. Using the state letter with a subscripted vibrational quantum number to denote a given level of an electronic state, this scheme indicated b_0 to be the immediate precursor of B_0, b_1 to be that for both B_1 and B_2 and b_2 to be that for B_3. We believe therefore that the fundamental mechanism of β band emission in $N(^4S)$ + $O(^3P)$ systems is now understood in terms of initial combination into high vibrational levels of $NO(a^4\Pi)$ with subsequent vibrational relaxation in this manifold and collision-induced crossings to near-isoenergetic $NO(b^4\Sigma^-)$ levels before further collision-induced crossing populates the corresponding $NO(B^2\Pi)$ levels.

However there is one interesting aspect of the β band behaviour in $N(^4S)$ + $O(^3P)$ systems which remains unexplained: the dramatic enhancement of emission intensities from B_1 and B_2 with increasing [O] above the basic [N][O] dependence. Preliminary work on these effects has been reported [3, 4], but, as will be shown in this paper, the interpretations advanced therein of the origins cannot be sustained. A new approach to the mechanism is now made on the basis of the results of an extensive series of observations of the kinetic behaviours of these emissions.

2. Experimental

The discharge–flow system used in this work has been described in detail before [4 - 6] so that only a brief resumé is necessary here.

A microwave discharge partially dissociated flowing N_2 well upstream of the observation tube. Total flow rates and pressures were in the ranges 100 - 1300 μmol s^{-1} and 0.1 - 1.4 kPa respectively. Titration and partial replacement of $N(^4S)$ atoms were achieved at a pepperpot jet just upstream of the observation section by addition of calibrated flow rates of NO and the very fast reaction

$$N(^4S) + NO \rightarrow N_2 + O(^3P)$$

In experiments involving mixed carrier gases, the other gases (Ar, CO_2) were added to the active nitrogen upstream of the pepperpot jet.

Chemiluminescent emission intensities were measured along the axis of the horizontal observation section from both ends. At the upstream end a collimated beam of radiation was detected using an EMI 6256B photomultiplier after passage through optical filters. Nitrogen first positive (1+) intensity ($\propto [N]^2$) was isolated using a Wratten 22 filter. Nitric oxide β band emissions ((1, 13) at about 413 nm and (2, 14) at about 421 nm) were isolated using tuned interference filters (Barr and Stroud Ltd.). At the down-

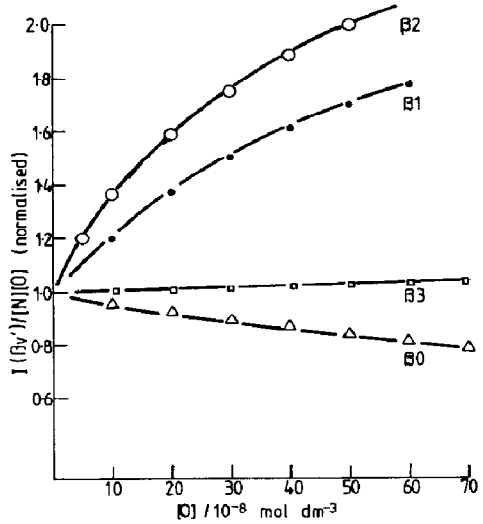

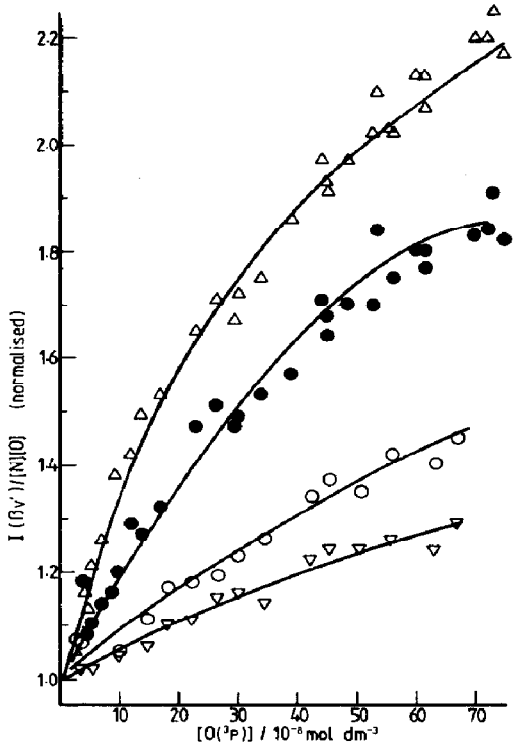

Fig. 1. The effect of increasing $[O(^3P)]$ on $I(\beta v')/[N][O]$ in pure N_2 at 298 K with [M] = 8×10^{-5} and [N] < 1×10^{-7} mol dm^{-3}: △, β_0; ●, β_1; ○, β_2; □, β_3.

Fig. 2. The effect of pressure on $I(\beta v')/[N][O]$ *vs.* [O] plots at 298 K and [N] = 1×10^{-8} mol dm^{-3}:

[M] (10^{-4} mol dm^{-3})	0.82	3.08
β_1	●	○
β_2	△	▽

stream end, radiation intensities were measured using another EMI 6256B photomultiplier mounted on the exit slit of a McPherson Model 218 monochromator purged with dry nitrogen. The grating had 2400 grooves mm^{-1} and was blazed for about 250 nm. The monochromator was used to measure individual band intensities of NO, principally the $\delta(0, 1)$ band at 198.0 nm and the $\beta(0, 5)$, (2, 4) and (3, 3) bands at 275.6 nm, 249.0 nm and 233.0 nm respectively. No band emanating from B_1 could be isolated in this region.

The $N(^4S)$ concentrations in the observation section were measured using the calibrated $N_2(1+)$ signals whilst $O(^3P)$ concentrations were calculated from the known flow rates of NO added. The tolerance of less than 5% decay of these concentrations along the observation tube was established as before [6]. Experiments were performed at room temperature (298 K) or at 195 K by surrounding the observation tube with crushed Cardice.

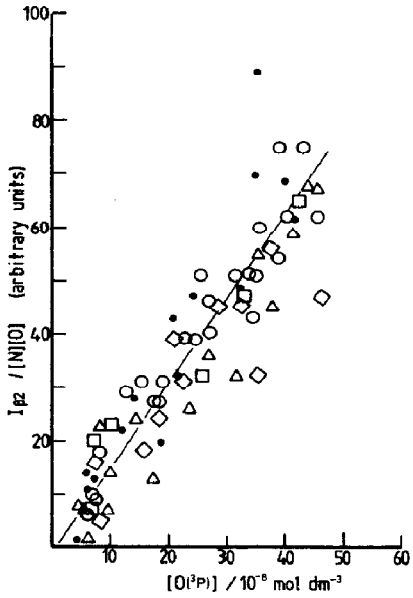

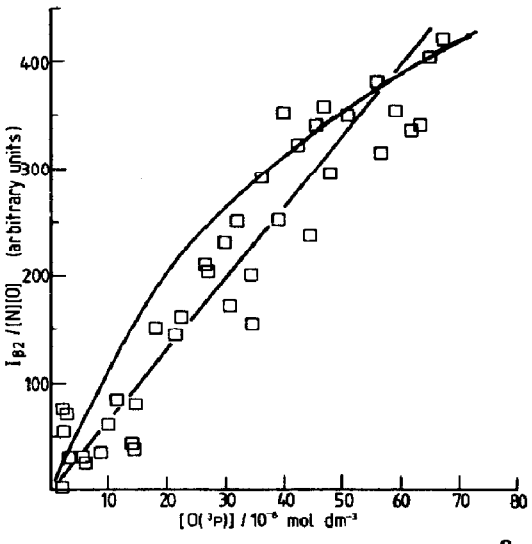

Fig. 3. The effect of pressure on $I_{\beta 2}$/[N][O] *vs.* [O] plots at 298 K and [N] = 1×10^{-8} mol dm^{-3}. [M] (10^{-4} mol dm^{-3}): ○, 0.61; ●, 1.08; △, 2.54; □, 4.3; ◇, 5.06.

Fig. 4. $I_{\beta 2}$/[N][O] *vs.* [O] at 298 K and [N] = 1×10^{-8} mol dm^{-3}. [M] (10^{-4} mol dm^{-3}): curved line, 0.82; □, 3.08.

As before the signals for a particular monochromator setting or optical filter were taken to be proportional to the integrated band intensity [6]. Again, the signal of the $\delta(0, 1)$ band ($I(\delta 0) \propto$ [N][O] and independent of [M] and carrier gas composition under our conditions) was adopted as an internal standard and the kinetic behaviours of the other bands were obtained from the ratios of their intensity to $I(\delta 0)$. For readings taken quickly in turn, this procedure reduces scatter due to any fluctuations of [N] and [O] on the time scale required to make a titration.

3. Results

3.1. O(^{3}P) enhancement effect in pure nitrogen carrier at 298 K

The measured β band signals $I(\beta v')$ were divided by $I(\delta 0)$ and plotted against [O] at constant [N] and [N_2]. Small back-extrapolations of these smooth plots then provided the intercepts $(I(\beta v')/I(\delta 0))_0$ for [O] = 0. These have been divided into the experimental $I(\beta v')$/[N][O] as shown in Fig. 1 which illustrates the effects of increasing [O] for all the β bands observed. It is evident that the bands originating from B_1 and B_2 are considerably enhanced by increasing [O] above the basic [N][O] dependence. In contrast, bands from B_0 and B_3 are both quenched slightly.

Figure 2 shows the effect of increasing [N_2] on the enhancements of B_1 and B_2 emissions. This illustrates the fundamental trends that the enhance-

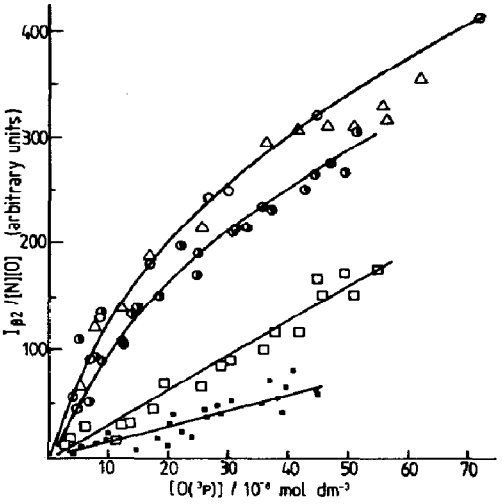

Fig. 5. The effect of quenchers on $I_{\beta 2}/[N][O]$ *vs.* [O] plots at 298 K and [N] = 1 × 10^{-7} mol dm^{-3}. Quencher: ○, pure N_2; △, 60% Ar–N_2; □, 10% CO_2–N_2; ■, 40% CO_2–N_2; ⊙, pure N_2 + [N] = 4.4 × 10^{-7} mol dm^{-3}.

ment effect tends to decrease with increasing $[N_2]$ and at the same time the curvature at low $[N_2]$ disappears effectively at high $[N_2]$. As will be drawn out in the discussion, there are two different population routes into B_1 and B_2. The basic route (for B_0, B_1, B_2 and B_3) involves a straightforward [N][O] proportionality of the population rate [6], the effect of which can be removed by simply subtracting $(I(\beta v')/I(\delta 0))_0$ from the measured $I(\beta v')/I(\delta 0)$ value, to leave a resultant value which we shall denote as $I_{\beta v'}/[N][O]$. Figure 3 then shows plots of this resultant parameter against [O] for a range of $[N_2]$.

This makes it very clear that the O atom enhancement effect is *largely* independent of N_2 pressure over the range 0.15 - 1.30 kPa at 298 K. The same is true for emission from B_1. However, the one effect of increasing N_2 pressure is re-emphasized in Fig. 4 in that distinct curvature appears at lower $[N_2]$. However *en masse* the data of Fig. 3 have the appearance of being scattered about a straight line. This will form the basis of the discussion to follow.

3.2. O(^{3}P) enhancement effects in mixed carriers at 298 K

Figure 5 shows the effect of various added gases on the residual parameter $I_{\beta v'}/[N][O]$. The inert gas argon has little effect until a very high mole fraction (at least 0.6) is reached when the only effect is an increased fall away from the N_2 curve at high [O]. At the same time it is shown that increased [N] in pure N_2 also leads to a similar effect but with the curves distinctly separated at rather lower [O] values. In contrast, CO_2 causes a dramatic linearizing of the plot while also reducing the scale of the enhancement effect. The gradient is reduced by increasing mole fractions of CO_2 although the relationship is evidently non-linear.

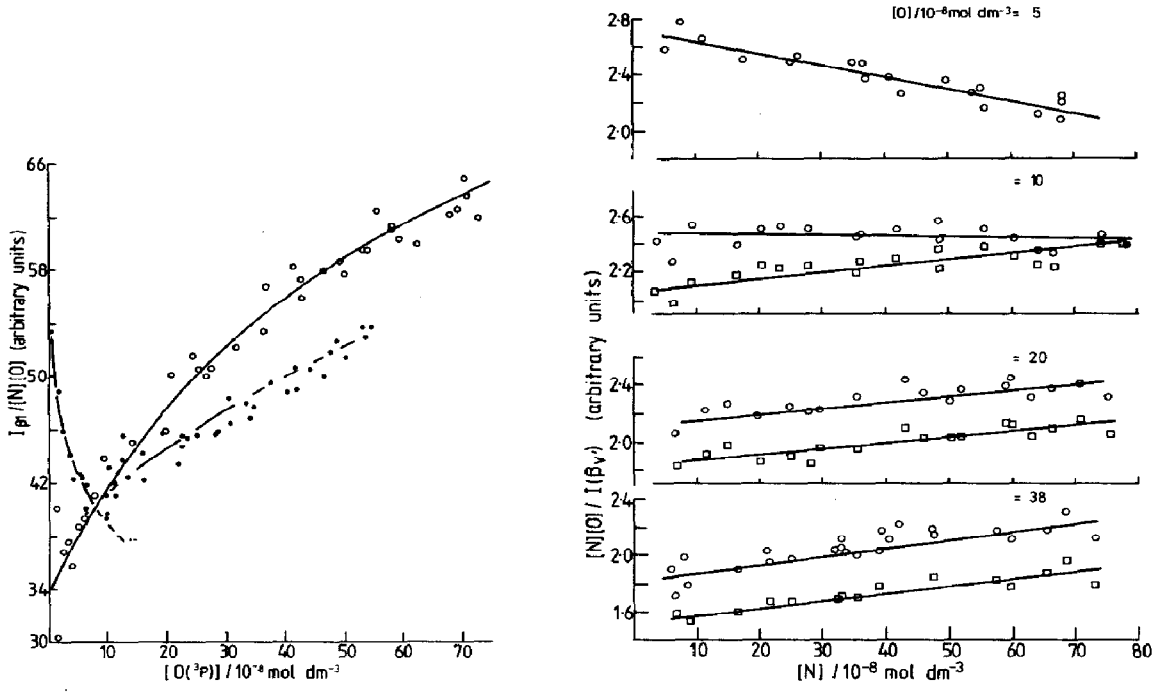

Fig. 6. The $\beta_{1,13}$ band $O(^3P)$ enhancement observed through the narrow band interference filter with various [N] at 298 K and [M] = 0.81×10^{-4} mol dm^{-3}. [N] (10^{-7} mol dm^{-3}): ○, 1; ●, 4.4.

Fig. 7. [N][O]/$I(\beta v')$ *vs.* [N] plots at different [O] showing the change from apparent enhancement to quenching by $N(^4S)$ at 298 K and [M] = 0.8×10^{-4} mol dm^{-3}: ○, β_1; □, β_2.

3.3. $O(^3P)$ enhancement effects in nitrogen at 195 K

As was pointed out before [4], the O atom enhancement effects on emissions from B_1 and B_2 are considerably greater at 195 K than at 298 K. Plots of the form of Fig. 3 have gradients increased by a factor of about 2 at 195 K for both emissions with no significant difference in the temperature coefficients.

3.4. [N] effects on "B_1 emission"

Light intensities measured through the interference filter tuned to about 413 nm (and thus the $\beta(1,13)$ band) appeared to show an N atom enhancement effect at low [O]. This is seen in Fig. 6 where values of $I_{\beta,1}$/[N][O] are plotted against [O] for different constant values of [N]. At low [N] the plot has the expected appearance but at high [N] a signal appears at [O] $\approx$ 0, which decreases rapidly at first on increasing [O] before eventually going over to an O atom enhancement effect which is quenched more than that at low [N]. This last feature is then very similar to the N atom quenching effect observed for the B_2 emission as detected by either the other

interference filter at about 421 nm (2, 14 band) or the monochromator at 249 nm (2, 4 band) which consequently is regarded as "normal behaviour".

The likely origin of the anomalous effect at low [O] and high [N] is that the "B_1 emission" as isolated by the filter includes some other emission whose intensity is likely to be proportional to some power of [N] higher than unity. At the same time it is clear that this other emission intensity is rapidly quenched by O atoms. Evidence supporting this interpretation is shown in Fig. 7 which shows the apparent [N] [O] /$I(\beta, 1)$ values plotted as a function of [N] at various [O]. At low [O], N atoms apparently enhance $I(\beta, 1)$, while as [O] increases the effect progressively turns over to a quenching. Plots of [N] [O] /$I(\beta, 2)$ are also included to emphasize that at the largest [O] the quenching effects have become very similar.

4. Discussion

A detailed basic mechanism of the excitation of β band chemiluminescence in N + O systems, in which the effects of atomic quenching or enhancement have been removed, has been given previously [1, 6]. The salient features are that the initial combination is into high levels of the vibrational manifold of NO($a^4\Pi$), followed by vibrational relaxation. There is a small leakage (about 4%) of the molecules due to collision-induced crossings in a reversible transverse manner into NO($b^4\Sigma^-$) followed by transverse crossings into levels of NO($B^2\Pi$) which are irreversible except in the case of B_3. At the pressures normally used for discharge–flow experiments subsequent losses from B_0, B_1, B_2 and B_3 are predominantly radiative.

We have postulated [1] that the closeness of matching of energy levels in the two states is the crucial factor determining the rate of $b_v \rightarrow B_{v'}$ crossings, with the ancillary factor of the wavefunction overlap. When the O atom enhancement of the intensities of bands originating from B_1 and B_2 was first reported it was suggested [3, 4] that the effects could be explained by O(^{3}P) atoms being more than three orders of magnitude more effective than $N_2(X^1\Sigma_g^+)$ in inducing the crossing $b^4\Sigma^- \rightarrow B^2\Pi$, which seemed feasible in the light of spin conservation requirements. However, following our recently improved knowledge of the relative energetic locations of b state levels [1, 5], there is no apparent reason why B_1 and B_2 should be favoured in this way while B_0 and B_3 are not. A further indication of the improbability of the original postulate is provided by the O atom enhancement effect on B_1 and B_2 observed when a quenching gas (*e.g.* CO_2 in Fig. 5) is present. The reduced enhancement effect seen in Fig. 5 would then suggest that CO_2 was more efficient than N_2 in inducing b → B crossing. However the results of our β band quenching experiments [6] in which the atom effects were extrapolated out of the data could not support this interpretation.

The results plotted in Fig. 2 are independent of the basic B state population mechanism described above. They are consistent with indepen-

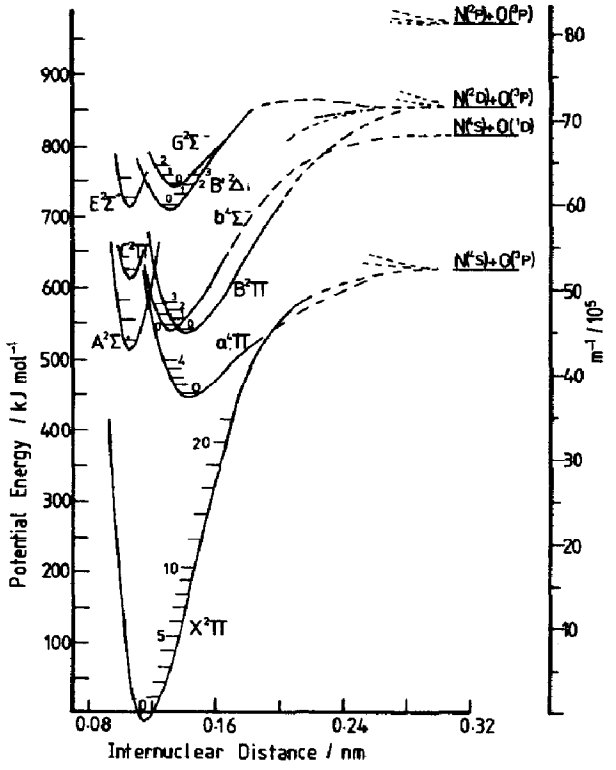

Fig. 8. Potential energy curves of nitric oxide.

dent rather than competitive paths. The *en masse* data of Fig. 3 indicate that the concentration $[B]_E$ of a particular B state level provided by the enhancement route is approximately described by

$$[B]_E = k_E[N][O]^2$$

The fact that the enhancement route appears to be highly specific to B_1 and B_2 suggests that its mechanism is likely to involve a step which depends strongly upon near-resonant energy transfer. The likelihood is that this is the step which forms B_1 and B_2 directly. Taking into account the general dependence derived from Fig. 3 that the intensity of emission from the enhancement route varies as $[N][O]^2$, the population step can be represented as

$$NO^* + O(^3P) \rightarrow NO(B_1, B_2) + O^* + \Delta E \qquad (1)$$

where NO* is an excited state of NO substantially above $D_0^0(NO)$, O* is an excited oxygen atom and ΔE is the energy converted to thermal energy and represents the difference from exact resonance. The potential energy diagram shown in Fig. 8 indicates two states of NO ($B'^2\Delta$ and $G^2\Sigma^-$) which could be identified with NO*, particularly because they lie almost directly above NO($B^2\Pi$) and also because they produce small ΔE values if O* is identified as O(^{1}D).

TABLE 1

The energy defects ΔE of the near-resonant processes
$O(^3P) + NO^*v' \rightarrow NO(B^2\Pi)v'' + O(^1D)$

$NO^* \equiv NO(B'^2\Delta)$[a]				
v'	1	2	3	4
v''	0	1	2	3
ΔE (kJ mol^{-1})	−2.08	−0.514	+0.801	+2.23
$NO^* \equiv NO(G^2\Sigma^-)$[b]				
v'	0	0	1	2
v''	0	1	2	3
ΔE (kJ mol^{-1})	+13.8	+(1.5 ± 1.1)	+(2.6 ± 1.1)	+(3.7 ± 1.1)

[a]Energy levels taken from ref. 7.
[b]Energy levels estimated from potential energy curves of ref. 8.

Table 1 shows values of ΔE calculated for transitions between rotationless vibrational levels which represent the most closely resonant process available to each B state level. For $NO(B'^2\Delta)$ as precursor it is clear that the resonance is considerably closer for populating B_1 and B_2 than it is for populating B_0 and B_3, just as is required to explain the specificity of the enhancement route. For $NO(G^2\Sigma)$ as precursor the situation is less clear because of the uncertainty in the exact energetic location of this state. Accordingly we shall pursue the argument further in general terms, with $NO(B'^2\Delta)$ $v' = 2,3$ indicated to be the most obvious identity of NO*.

From the kinetic dependence of the enhancement route intensity it is then clear that [NO*] must vary simply as [N][O], while at the same time we must introduce some component of the mechanism to explain the curved plot of Fig. 4 at lower pressures. Let us assume for the moment that the population rate of NO* is k_1[N][O][M] (justified later). If the subsequent mechanism is

$$O(^3P) + NO^* \rightarrow NO(B_{1,2}) + O(^1D) \quad (2)$$

$$NO^* + M \rightarrow \text{non-emitting states} \quad (3)$$

$$NO(B_{1,2}) \rightarrow NO(X) + h\nu \quad (4)$$

then steady state analysis yields the intensity I_β originating from the enhancement route:

$$\frac{I_\beta}{[N][O]} = \frac{k_1 k_2\,[O][M]}{k_2[O] + k_3[M]} \quad (I)$$

At high [M] where k_3[M] $\gg$ k_2[O] this leads simply to a linear variation of I_β/[N][O] with [O] as observed. Also if CO_2 is more efficient than N_2

in step (3) then a quenched linear variation at lower [M] is predicted, also as observed. At low $[N_2]$, if $k_3[N_2]$ is not too much larger than $k_2[O]$, eqn. (I) predicts the curvature observed.

We must now calculate the effective value of k_1 to see whether it is reasonable. It has been established [4] that about 4% of N + O combinations lead to NO(B) and in the absence of atom enhancement effects at 298 K only about 10% of this leads to $NO(B_1, B_2)$. From data shown in Fig. 2, with conditions of $[N_2] = 8 \times 10^{-5}$ mol dm^{-3}, $[N] = 1 \times 10^{-7}$ mol dm^{-3}, extrapolation of the linear onsets shows that for $[O] \approx 3 \times 10^{-7}$ mol dm^{-3} the rate of passage through NO* must be at least equal to the rate of passage into $NO(B_1, B_2)$ by the basic route. Since the overall rate constant for N + O combination at 298 K is 3.3×10^9 dm^6 mol^{-2} s^{-1} [9] and about 0.4% of the combinations populate B_1 and B_2 by the basic mechanism, this means that from eqn. (I)

$$k_1 k_2[O]/k_3 \geqslant 2 \times 10^7[N_2] \qquad \text{(II)}$$

Since at $[O] = 3 \times 10^{-7}$ mol dm^{-3} the actual points are about 10% below the extrapolated linear onset, $k_2[O] \approx 0.1\ k_3[N_2]$, so that on inserting the values we derive $k_2/k_3 \approx 27$. Substitution into eqn. (II) leads to

$$k_1 \geqslant 1.3 \times 10^8 \text{ dm}^6 \text{ mol}^{-2} \text{ s}^{-1}$$

Such a value is not unreasonable in the light of the mechanism given later for excitation of NO*.

The most likely mechanism for the generation of an NO* species with energy well above $D_0^0(NO)$ must involve the excited atomic species $N(^2D)$, $N(^2P)$, $O(^1S)$ or $O(^1D)$, since we see from Fig. 8 that this opens up the possibility of combination into NO(B′, G) with the aid of curve crossing processes. Therefore at this point it is relevant to discuss the possibilities for atomic electronic excitation in N + O systems.

4.1. Atomic electronic excitation mechanisms

In the first place it can be pointed out that no significant concentrations of excited atoms could have survived the flowtime of at least 0.1 s from the discharge region to the observation section. In active nitrogen itself $N(^4S)$ atoms induce a major quenching process on $N_2(A^3\Sigma_u^+)$ formed by N + N combination and the formation of $N(^2P)$ in the process

$$N(^4S) + N_2(A^3\Sigma_u^+)\ (v' = 0, 1) \rightarrow N(^2P) + N_2(X^1\Sigma_g^+)$$

has been measured [10] to occur with a collisional efficiency of about 20%. About half this efficiency attaches to the process

$$O(^3P) + N_2(A^3\Sigma_u^+)\ (v' = 0, 1) \rightarrow O(^1S) + N_2(X^1\Sigma_g^+)$$

However, Table 2 shows that on the grounds of energy resonance $N(^2D)$ and $O(^1D)$, rather than $N(^2P)$ and $O(^1S)$, are the favoured products. The fact that neither $N(^2D)$ nor $O(^1D)$ were actually observed in emission by Meyer *et al.* [10] can probably be ascribed to their long radiative lifetimes of 26 h

TABLE 2

The energy deficit ΔE of the near-resonant processes
$N(^4S), O(^3P) + N_2(A^3\Sigma_u^+)v' \rightarrow N^*, O^* + N_2(X^1\Sigma_g^+)v''$

N*, O*	$N(^2D)$	$O(^1D)$	$O(^1S)$	$O(^1D)$	$N(^2P)$
v'	1	0	0	1	1
v''	15	16	7	17	10
ΔE (kJ mol^{-1})	+0.65	+1.2	−3.3	−4.1	+4.2

($N(^2D)$) and 100 s ($O(^1D)$) as opposed to 12 s ($N(^2P)$) and 7 s ($O(^1S)$), which also in combination with known rate constants for quenching by N_2 (see Table 5 to follow) would mean that the overwhelming majority of $N(^2D)$ and $O(^1D)$ atoms would have been quenched in these experiments. It is therefore quite possible that energy resonance is a critical factor in the interaction of $N(^4S)$ and $O(^3P)$ atoms with $N_2(A^3\Sigma_u^+)$.

Campbell and Neal [4] found that in N + O systems β band emission from B_0 in particular was quenched by $N(^4S)$ and $O(^3P)$ atoms. Detailed examination of the kinetics showed that the N atom quenching was due to interaction of $N(^4S)$ with the immediate precursor of B_0, postulated as b_0 [1], whilst the O atom quenching was due to direct interaction with B_0. Table 3 identifies possible near-resonant energy transfer processes for these interactions, represented as

$$N(^4S), O(^3P) + NO(B,b)v' \rightarrow N^*, O^* + NO(X^2\Pi)v''$$

The energy of b_0 was taken as 547.1 kJ mol^{-1} above $NO(X^2\Pi)$ $v'' = 0$ [1]. The absolute quenching rate constants shown in the last column are based on the radiative lifetime measurements of Jeunehomme [12] and are assigned to the reaction indicated on the basis that the most resonant process makes the greatest contribution to the quenching observed. Table 3 shows that close resonances are achieved for the processes

$$O(^3P) + NO(B_0) \rightarrow O(^1D) + NO(X)v'' = 18$$

$$N(^4S) + NO(b_0) \rightarrow N(^2D) + NO(X)v'' = 16$$

and the magnitudes of ΔE for these processes are significantly smaller than those for most of the other processes listed. The table suggests N atoms may interact directly with B_1 at a significant rate, but our present data are insufficient to investigate this point. Hence it appears that the energy resonance approach can interpret the observations in this case.

The most abundant electronically excited species in N + O systems is likely to be $NO(a^4\Pi)$ since statistically this state should be populated by 67% of combinations. There is no reason to suppose that N_2 will quench this species efficiently since the lower vibrational levels have insufficient

TABLE 3

The energy defects ΔE and available rate constants k_q for quenching of the near-resonant processes

$$N(^4S), O(^3P) + NO(B, b)v' \rightarrow N^*, O^* + NO(X^2\Pi)v''$$

N*, O*	B, v'	b, v'	v''	ΔE (kJ mol^{-1})	$10^{-10}k_q$ (dm^3 mol^{-1} s^{-1})	
$O(^1D)$	0		18	+0.38	9.2	[11]
$N(^2P)$	1		10	+0.61	—	
$N(^2D)$		0	16	−0.77	$4k$	[11]
$O(^1D)$		2	20	+0.97	—	
$N(^2D)$	2		17	+1.2	—	
$O(^1S)$		2	8	+1.2	—	
$N(^2P)$		2	11	+2.2	—	
$N(^2D)$	3		18	−2.3	<8	[11]
$O(^1D)$	1		19	−2.4	—	
$N(^2D)$		1	17	−3.2	—	
$O(^1D)$		1	19	+2.9	—	
$O(^1D)$		0	18	+4.3	k	[11]
$O(^1D)$	3		20	+4.3	—	
$N(^2D)$	0		16	−4.6	1.3	[11]

energy to produce any electronically excited state of N_2 by direct transfer. Therefore, by analogy with $N_2(A^3\Sigma_u^+)$ quenching in active nitrogen we propose that potential near-energy resonances will make it likely that a substantial part of $NO(a^4\Pi)$ is removed by energy transfer to $N(^4S)$ and $O(^3P)$ atoms. This proposal must be tempered with the probability that $N(^4S)$ atoms can also react chemically

$$N(^4S) + NO(a^4\Pi) \rightarrow N_2 + O$$

by analogy with the ground state NO reaction which proceeds at around 10% of the collision frequency. However, as pointed out earlier, in the case of $N_2(A^3\Sigma_u^+)$ the energy transfer reactions with $N(^4S)$ and $O(^3P)$ to produce $N(^2P)$ and $O(^1S)$ respectively involve quite large ΔE (Table 2) and yet proceed at 10% or more of the collision frequency. It might therefore be expected that more nearly resonant processes in the case of $NO(a^4\Pi)$ would dominate chemical reaction. Table 4 shows that this situation can be achieved in that there are many opportunities for near-resonant energy transfer, particularly for N atom interaction. The table is based on our location [1] of the rotationless $NO(a^4\Pi)v' = 0$ level at an energy of 453.6 kJ mol^{-1} above $NO(X^2\Pi)v'' = 0$ and includes levels $v' \leqslant 4$.

In conclusion to this section, we regard it as highly reasonable to regard a substantial fraction of $NO(a^4\Pi)$ molecules formed in N + O systems as generating $N(^2P, ^2D)$ and $O(^1S, ^1D)$ atoms by energy transfer.

TABLE 4

The energy defects ΔE of the near-resonant processes
$N(^4S), O(^3P) + NO(a^4\Pi)v' \rightarrow N^*, O^* + NO(X^2\Pi)v''$

N*, O*	$N(^2P)$	$N(^2P)$	$N(^2D)$	$O(^1D)$	$O(^1D)$	$O(^1S)$
v'	0	2	2	2	0	0
v''	5	6	12	14	13	2
ΔE (kJ mol)	−0.43	+0.67	−0.81	+1.9	−1.9	+3.1

TABLE 5

Quenching rate constants for electronically excited atoms[a]

Quencher	$N(^2D)$	$N(^2P)$	$O(^1D)$	$O(^1S)$
N_2	9.0×10^6 [13]	6×10^4 [13]	1.7×10^{10} [14]	$<1.2 \times 10^5$ [15]
CO_2	1.1×10^8 [13]	6.6×10^5 [13]	6.0×10^{10} [14]	2.2×10^8 [15]
$N(^4S)$	—	3.7×10^8 [16]	—	$\leqslant 6 \times 10^8$ [17]
$O(^3P)$	1×10^9 [18]	6.0×10^9 [16]	—	4.5×10^9 [17]

[a]The values listed are expressed as $dm^3\ mol^{-1}\ s^{-1}$ at 298 K.

4.2. Proposed mechanism of $NO(B'^2\Delta)$ formation

Any one of $N(^2P, ^2D)$ or $O(^1S, ^1D)$ could provide sufficient energy for the combination with $O(^3P)$ or $N(^4S)$ respectively to populate $NO(B'^2\Delta)v' \leqslant 3$ (Fig. 8). However, once formed, the excited atoms will be subject to quenching by the carrier gas. Table 5 summarizes available values of the relevant quenching rate constants.

Under our conditions ($[N_2] \geqslant 8 \times 10^{-5}$ mol dm^{-3}) it can be seen that $O(^1D)$ will be rapidly quenched by N_2 and although $N(^2D)$ is less efficiently quenched both of these can be considered to be unlikely to survive long enough to take a substantial part in a combination process. In contrast, $N(^2P)$, the species apparently most favoured by the ΔE value in Table 4, appears to fulfill the required role since it reacts very rapidly with $O(^3P)$ but is not subject to significant quenching by N_2. Figure 8 shows that the energy of $N(^2P) + O(^3P)$ is considerably higher than $NO(B'^2\Delta)v' = 2, 3$. However, there are many intersecting potential curves of NO states at these high energies, of uncertain location in many cases, which cannot be shown in Fig. 8; thus there would appear to be little problem in postulating that the initial species formed by $N(^2P) + O(^3P)$ find their way, to some extent, via energy removal and curve crossing processes to $NO(B'^2\Delta)(NO^*)$. Thus we are proposing the effective mechanism

$$N + O + M \rightarrow NO(a^4\Pi) + M \qquad (a)$$

$$N(^4S) + NO(a^4\Pi) \rightarrow N(^2P) + NO \quad (b)$$

$$N(^2P) + O(^3P) \rightarrow NO^{**} \quad (c)$$

$$NO^{**} + M \rightarrow NO^{*} + M \quad (d)$$

$$NO^{**} + M \rightarrow \text{other products} \quad (e)$$

where NO** is the initially populated high energy state.

On the basis of the resonance considerations and the values of ΔE shown in Table 4 it would not be unreasonable to suggest that process (b) dominates the removal of $NO(a^4\Pi)$ so that the rate of production of $N(^2P)$ is approximately equal to $k_a[N][O][M]$ and $[N(^2P)] = (k_a/k_c)[N][M]$. Applying further stationary state considerations we obtain

$$[NO^{**}] = k_a[N][O]/(k_d + k_e)$$

and the rate of production of NO* is given by

$$\frac{k_d k_a [N][O][M]}{k_d + k_e}$$

Thus k_1 which we defined earlier in the paper and assessed as $\geqslant 1.3 \times 10^8$ $dm^6\ mol^{-2}\ s^{-1}$ is equated to $k_d k_a/(k_d + k_e)$. The upper limit on k_a on statistical grounds, and taking the overall N + O + M combination rate constant as $3.3 \times 10^9\ dm^6\ mol^{-2}\ s^{-1}$, is $2.2 \times 10^9\ dm^6\ mol^{-2}\ s^{-1}$. Thus we require $k_d/(k_d + k_e)$ to be a lower limit of about 0.06. This imposes no unrealistic demand on the above mechanism since it fully takes account of the likelihood that relatively little of NO** is converted to NO* and/or allows process (c) to be one of a set of parallel processes.

Whilst the above mechanism involves some rather sweeping assumptions, we nevertheless feel that it must be considered as the main mechanism of the enhancement route.

4.3. The apparent N atom enhancement of "B_1 emission"

The "B_1 emission" as detected by the interference filter at about 413 nm (band width 2.0 nm) contains an additional component to the (1, 13) β band which is particularly emphasized at high [N] (Fig. 6). Since the intensity of this underlying emission must vary as $[N]^x$ with $x > 1$, we argue that it is likely to be an N_2 emission band. However, when the monochromator was used to scan this spectral region under similar conditions to those for Figure 6 (*i.e.* $[N] > 4 \times 10^{-7}$ mol dm^{-3}, $[O] < 0.5 \times 10^{-7}$ mol dm^{-3}) no clear structure was seen underlying the NO $\beta(1, 13)$ band as shown in Fig. 9.

However, it must be pointed out that these scans are made with relatively wide slits since the intensity is low: also it is not helpful that the effect is most notable at small [O]. At the same time it must be borne in mind that the effect of the additional emission is small with $I(\beta, 1)/[N][O]$ only increasing by about 25% on this account under the most favourable conditions, as shown in Figure 7. The transmission characteristics of the two interference filters are shown in Fig. 9 and it must be borne in mind that no anomalous N atom enhancement effects were found for the B_2 emission.

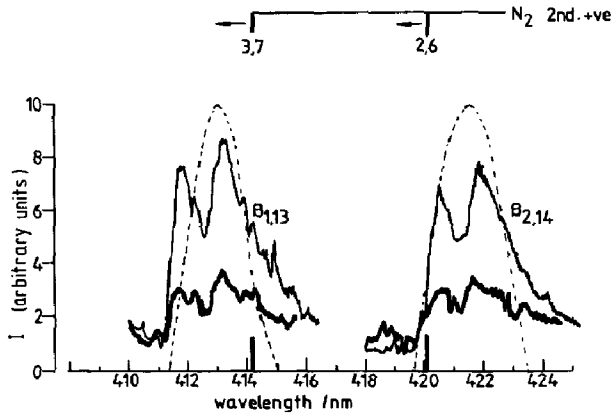

Fig. 9. Monochromator scans of the $\beta_{1,13}$ and $\beta_{2,14}$ bands at 298 K, [M] = 0.8×10^{-4} mol dm^{-3}, [N] > 4×10^{-7} mol dm^{-3} and a slit width of 500 μm. [O] (10^{-7} mol dm^{-3}): narrow line, 1; broad line, less than 0.2. The transmission windows of interference filters centred at 413 and 421 nm (broken lines) and the positions of overlapping N_2 2nd + ve bands are also shown.

We believe that the most likely origin of the additional emission is N_2 second positive (2+) bands ($C^3\Pi_u \rightarrow B^3\Pi_g$). The (3, 7) band with head at 414.2 nm and (2, 6) band with head at 420.1 nm are known to be excited in nitrogen discharges, by energy pooling of $N_2(A^3\Sigma_u^+)$ molecules [16] and, more importantly in the present case, it has been suggested that $N_2(C^3\Pi_g)$ is populated by combination of $N(^2P)$ and $N(^4S)$ atoms [13]. These bands are degraded to the blue and the indicated band head positions in Fig. 9 show that, while the (3, 7) 2+ band lies almost completely within the B_1 filter transmission window, the (2, 6) 2+ band will be substantially outside the B_2 filter transmission window: thus the incursion of 2+ signal into "B_1 emission" but its absence from "B_2 emission" as detected by the filters is to be expected if 2+ emission is excited significantly.

The involvement of $N(^2P)$ in the excitation mechanism of the 2+ band emission fits well with the knowledge that $N(^2P)$ is rapidly removed by interaction with $O(^3P)$. In Fig. 6, the high [N] data for B_1 emission is then resolved into two segments with increasing [O]: on the most obvious basis the left-hand segment reflects the sharp decrease of concentration of the $N(^2P)$ precursor species as [O] increases while the right-hand segment back-extrapolates to reflect the simultaneous appearance of the product species B_1, produced by the enhancement route. This being the case, we can admit our good fortune in having been able to find the complementary effects using one filter.

5. Conclusion

We have investigated the oxygen atom enhancement effect on β band emissions from $NO(B^2\Pi)v' = 1, 2$ and have shown that it can be explained

through a mechanism where energy transfer from NO($a^4\Pi$) molecules to N(^{4}S) atoms generates N(^{2}P) atoms and these combine with O(^{3}P) atoms to yield a state NO($B'^2\Delta$) with energy well above D_0^0(NO). The subsequent energy transfer from NO($B'^2\Delta$) to O(^{3}P) leads to NO($B^2\Pi$)$v' = 1, 2$ and O(^{1}D). The specificity of these energy transfer processes derives strongly from the closeness to energy resonance. Similar energy resonance considerations allow interpretation of the direct quenching of NO($B^2\Pi$)$v' = 0$ by O(^{3}P) atoms and the quenching of its NO($b^4\Sigma^-$)$v' = 0$ precursor by N(^{4}S) atoms as predominant effects.

References

1 I. M. Campbell and R. S. Mason, *J. Photochem., 8,* (1978) 375.
2 D. Vichon, R. I. Hall, F. Gasteau and J. Mazeau, *J. Mol. Spectrosc., 69* (1978) 341.
3 I. M. Campbell, S. B. Neal, M. F. Golde and B. A. Thrush, *Chem. Phys. Lett., 6* (1971) 612.
4 I. M. Campbell and S. B. Neal, *Discuss. Faraday Soc., 53* (1972) 72.
5 I. M. Campbell and R. S. Mason, *J. Photochem., 5* (1976) 383.
6 I. M. Campbell and R. S. Mason, *J. Photochem., 8* (1978) 321.
7 J. T. Vanderslice and E. A. Mason, *J. Chem. Phys., 30* (1959) 129.
8 F. R. Gilmore, *J. Quant. Spectrosc. Radiat. Transfer, 5* (1965) 369.
9 I. M. Campbell and C. N. Gray, *Chem. Phys. Lett., 18* (1973) 607.
10 J. A. Meyer, D. W. Setser and D. H. Stedman, *J. Phys. Chem., 74* (1970) 2238.
11 S. B. Neal, *Ph.D. Thesis,* University of Leeds, 1976.
12 M. Jeunehomme and A. B. F. Duncan, *J. Chem. Phys., 41* (1964) 1692.
13 D. Husain, S. K. Mitra and A. N. Young, *J. Chem. Soc. Faraday Trans. II, 70* (1974) 1721.
14 J. A. Davidson, H. I. Schiff, G. E. Streit, J. R. McAfee, A. L. Schmeltekopf and C. J. Howard, *J. Chem. Phys., 67* (1977) 5021.
15 S. V. Filseth, F. Stuhl and K. H. Welge, *J. Chem. Phys., 52* (1970) 239.
16 R. A. Young and O. J. Dunn, *J. Chem. Phys., 63* (1975) 1150.
17 W. Felder and R. A. Young, *J. Chem. Phys., 56,* (1972) 6028.
18 J. E. Davenport, J. G. Slanger and G. Black, *J. Geophys. Res., 81* (1976) 12.
19 G. N. Hays, C. J. Tracy, A. R. Demonchy and H. J. Oskam, *Chem. Phys. Lett., 14* (1972) 352.